A FULL ANALYTICAL METHOD TO DETERMINE EQUILIBRIUM QUANTITIES OF MISMATCHED CHARGED PARTICLE BEAMS EVOLVING IN LINEAR CHANNELS*

R. P. Nunes#, F. B. Rizzato†
Instituto de Física, UFRGS, Av. Bento Gonçalves 9500, C.P. 15051, Porto Alegre, Brasil

Abstract

The focus of this work is to show a full analytical expression to determine relevant equilibrium quantities of a magnetically focused and high-intensity charged particle beam when evolving in a linear channel. Through the current approach, some intermediate steps of our original hybrid model which have to be solved numerically now can be eliminated, leading to the obtainment of a full analytical expression. This expression relates initial beam parameters with those obtained at equilibrium, allowing that the fraction of halo particles f can be evaluated. As a consequence, through the developed model, beam quantities like the envelope and emittance can be naturally determined. This is important in the accelerator engineering, since halo characteristics is a factor to be considered in the design of its confinement structure. For validation, full self-consistent N-particle beam numerical simulations have been carried out and its results compared with the predictions supplied by the full analytical model. The agreement is shown to be nice as with the simulations as with the hybrid numerical-analytical version of the model.

INTRODUCTION

As charged beams evolve inside the focusing channel, some small quantity of its particles are ejected, developing large amplitude orbits much different from those plasma-like orbits performed by the remaining particles. Although small, its contribution over the calculation of statistically-averaged beam quantities becomes to be important so more as the equilibrium approaches. At equilibrium, observing the beam configuration space, it is possible to detect that the initially spatial-limited particle population is now surrounded by a tenuous particle population. This tenuous population is dispersed in such a way that its influence over the beam cannot be neglected anymore, being named as halo in beam physics. This behavior is observed in self-consistent N-particle beam numerical simulations [1] as well as in the experiments [2]. In this way, halo formation has become a subject extensively studied in beam physics, and its effects over the infrastructure of the accelerator a problem to be mitigated in engineering.

Macroscopically, the particle ejection commented above is perceived as the change of two statistical-average quantities of the beam distribution during its excursion inside the focusing channel. One is the beam envelope r_b, which appreciates an important decay, and the other is the beam emittance ϵ, which experiences additionally a not negligible growth. The beam envelope and emittance have an inverse dynamical behavior (the first decay, the second grow) not for coincidence, but because they are concatenated by a constraint: energy conservation. The beam distribution evolves assuming that its overall energy remains constant. In this way, if the beam envelope decays (potential energy decreases), then emittance must grow (kinetic energy increases), because the overall energy inevitably conserves. The striking characteristic observed here is that almost all beam kinetic energy is carried by a small amount of particles. Since emittance and kinetic energy are directly connected, the tenuous population has therefore great importance in the emittance growth during the focusing process.

This progressive increasing of beam kinetic energy is proportioned by the interaction of individual particles with the mismatched beam. As beam propagates inside the focusing channel, its envelope mismatch induces the formation of large resonant islands [3] beyond its border. Individual particles are captured by this resonance [4], coupling their motion with the mismatched beam. The resonant coupling — fruit of the particle-beam interaction — is the way that energy exchange occurs: potential energy of the beam oscillatory motion is converted into kinetic energy that supplies the chaotic movement of the individual particles. Equilibrium is reached when this energy transfer mechanism ceases. Together, all other commented statistically-averaged quantities also stabilize. At this point, it is of interest to known which values achieve the envelope r_b and emittance ϵ, not only for physics purpose but also for engineering aspects, associated to the design of the confinement structure.

The system considered here is a high-intensity beam of charged particles, focused by a constant magnetic field in a linear propagation channel. The initial beam density is considered homogeneous, being described by a step-function profile

$$n(r, s=0) = \begin{cases} N/\pi r_o^2, & \text{for } 0 \le r \le r_b \\ 0, & \text{for } r_b < r \le r_w \end{cases}, \tag{1}$$

where r_w is the conduct pipe location and r_o designates the initial beam mismatch. Azimuthal symmetry is also assumed for simplification.

THE DEVELOPED MODEL

In Figure 1, it is shown several snapshots of the beam transverse phase-space after equilibrium is attained. It is possible to observe that the equilibrium is directly associated to the invariance of phase-space topology.

*CNPq and FAPERGS, Brazil.
#rogerpn@if.ufrgs.br, †rizzato@if.ufrgs.br

Particle orbits are defined in such a way that they occupy a well-defined and limited region in the phase-space. In each of these regions, the number of particles remains almost constant. This is the reason by which statistically-averaged quantities of the beam distribution stabilize at the equilibrium. In average, the microscopic states (composed by the coordinates of each particle in the phase-space) do not considerably change. Since, macroscopic quantities are just averages over the microscopic states, thus envelope and emittance do not experience any alteration in its values. The results obtained in Figure 1 are from self-consistent N-particle beam simulations using Gauss' Law [1].

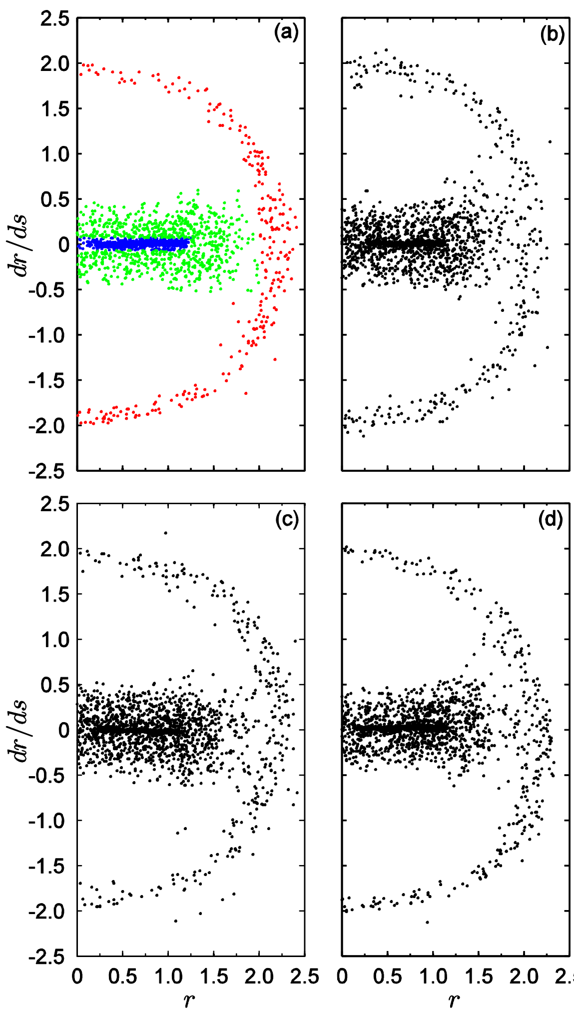

Figure 1: Snapshots of the beam transverse phase-space at its equilibrium for an initial envelope mismatch of $r_o = 1.5$. Phase-space topology invariance is attained. Phase-space portraits captured at (a) $s = 547{,}8$, (b) $s = 599{,}7$, (c) $s = 798{,}7$, and (d) $s = 997{,}6$.

The beam phase-space at equilibrium can be decomposed in three regions: a horizontal thin branch, composed by very cold particles, a cloud around the horizontal branch, made up of warm particles, and by a semicircular branch, populated by extremely hot particles. Although warm particles have fundamental role in halo formation, thus important for the description of the beam transient behavior, their contribution at equilibrium can be neglected. As an approximation, they can be considered as cold particles [5]. In this way, it is possible to associate the cold particles to the core as well as the hot ones with those that compose the halo. In Figure 1(a), the cold, warm, and hot particles appear detached in respectively blue, green, and red.

The regular geometry of each previously commented regions of the beam phase-space can be directly converted to analytical expressions. At equilibrium, beam density assumes [6]

$$n(r) = \begin{cases} n_c(r) + n_h(r), & \text{for } 0 \le r \le r_c \\ n_h(r), & \text{for } r_c < r \le r_h \\ 0, & \text{for } r_h < r \le r_w \end{cases}, \tag{2}$$

where n_c and n_h are respectively the particle density for the core and the halo, r_c is the core size and r_h is associated with the size projected by the semicircular branch over r axis.

The core population at equilibrium can be still represented as step-function profile [6]

$$n_c(r) = (1-f)N/\pi r_c^2, \tag{3}$$

now with $r_c < r_o$ and expressed by fraction $f \equiv N_h/N$ through the relation $N = N_c + N_h$. The halo population pertaining to the semicircular branch follows [6]

$$n_h(r) = \frac{fN}{\pi^2 r\sqrt{r_h^2 - r^2}}. \tag{4}$$

Inserting equations (3) and (4) into equation (2) the equilibrium is completely defined. With the beam density, it is possible to determine its self-consistent generated electric field $\mathbf{E}$ by the means of the following Maxwell equation [7]

$$\nabla \cdot \mathbf{E} = -\frac{2\pi K}{N} n(\mathbf{r}). \tag{5}$$

in which K is the beam perveance. Doing that, one obtains the expression for $\mathbf{E}$

$$E(r) = \begin{cases} -\frac{(1-f)r}{r_c^2} - \frac{2f}{\pi r}\tan^{-1}\left(\frac{r}{\sqrt{r_h^2 - r^2}}\right), & \text{for } 0 \le r \le r_c \\ -\frac{2f}{\pi r}\tan^{-1}\left(\frac{R}{\sqrt{r_h^2 - r^2}}\right) - \frac{(1-f)}{r}, & \text{for } r_c < r \le r_h \\ -\frac{1}{r}, & \text{for } r_h < r \le r_w \end{cases}. \tag{6}$$

The overall beam energy can be computed at any instant of time s through [6]

$$\frac{r_b^2(s)}{2} - \frac{1}{4} + \mathcal{E}(s) = E = constant, \tag{7}$$

in which $\mathcal{E}$ is the average self-field beam energy [7]

$$\mathcal{E}(s) = \frac{1}{4\pi K}\int |\mathbf{E}|^2 d\mathbf{r}. \tag{8}$$

The beam envelope r_b at equilibrium assumes in the semicircular approximation the form [6]

$$r_b^2 = (1-f)r_c^2 + f r_h^2. \tag{9}$$

Inserting equations (8) and (9) into equation (7), the beam energy at equilibrium is obtained. Proceeding in the same form with the initial density of equation (1), it is possible also to evaluate energy at the beginning. It becomes possible thus to connect both recently obtained expressions, generating an equation for fraction f. This equation is a second-order polynomial [6]

$$Af^2 + Bf + C = 0, \tag{10}$$

which the desired solution resides between $0 \leq f \leq 1$.

The average self-field beam energy depends on the square value of the electric field. For this reason, an exact analytical solution to the coefficients of the polynomial in equation (10) is difficult. Nevertheless, with the following approximation for the inverse tangent [8]

$$\tan^{-1}\left(\frac{r}{\sqrt{r_h^2 - r^2}}\right) \approx \frac{3(r/r_h)}{2 + \sqrt{1 - (r/r_h)^2}}, \tag{11}$$

after exhaustive algebra the coefficients A, B e C of the polynomial in equation (10) can be written as [5]

$$\begin{aligned} A(r_c, r_h) &\approx \varsigma + \ln(r_c^2/r_h^2) - [72\ln(2/3) + 24]/\pi^2 - 1/2 \\ B(r_c, r_h) &\approx -\varsigma + 2\ln(r_c^2/r_h^2) + 1 + 2(r_c^2 - r_h^2) \\ C(r_o, r_c) &\approx 1 - 2r_c^2 + r_o^2 + \ln(r_c^2/r_o^2) \end{aligned} \tag{12}$$

in which ς is the auxiliary equation below

$$\begin{aligned} \varsigma(r_c, r_h) = &-\left[\frac{48 r_h^2\sqrt{3}}{\pi r_c^2} + \frac{16\sqrt{3}}{\pi}\right]\tan^{-1}\left[\frac{\sqrt{3}r_h}{3r_c}\left(1 + 2\sqrt{1 - \frac{r_c^2}{r_h^2}}\right)\right] \\ &+ \left[\frac{84 r_h^2}{r_c^2} + \frac{24}{\pi}\right]\sin^{-1}\left(\sqrt{1 - \frac{r_c^2}{r_h^2}}\right) \\ &- \frac{48 - 12\sqrt{1 - \frac{r_c^2}{r_h^2}}}{\pi r_c/r_h} + \frac{24\sqrt{3} - 42}{r_c^2/r_h^2} + \frac{8\sqrt{3}}{2}. \end{aligned} \tag{13}$$

Comparison between the inverse tangent and its approximation of equation (11) is shown in Figure 2. There is a visible divergence between both expressions just as $r/r_h \to 1$.

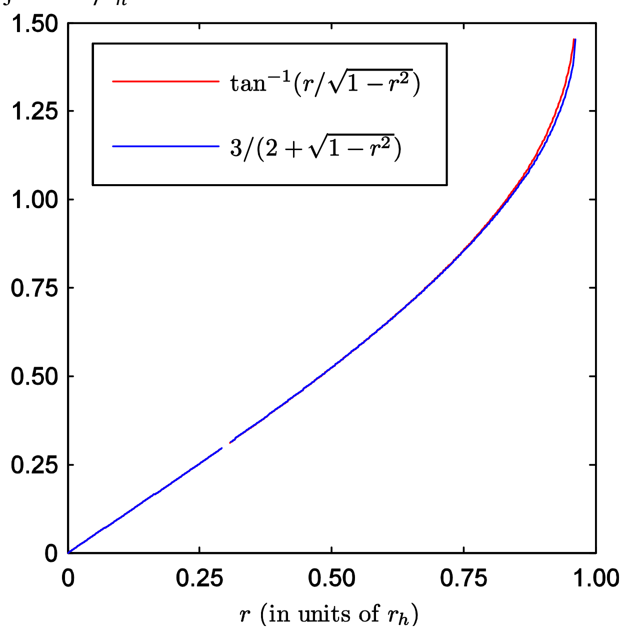

Figure 2: Comparison between the inverse tangent function and its approximation adopted to solve analytically the integrals.

RESULTS

The results obtained with the model through both the numerical solution and the quasi-exact analytical solution is shown in Table 1. Also in this table, the results provided by the full N-particle numerical simulations is shown. The comparison of the results occurs for the fraction of halo particles f, the envelope r_b, and the emittance ϵ at equilibrium. The columns explicit the results for each analyzed mismatch r_o. The first two rows show the beam phase-space parameters at equilibrium, necessary to evaluate the previously commented beam quantities. Results obtained from the quasi-exact analytical model is almost the same that the ones computed by numerical solution of equation (10).

Table 1: The results obtained through the developed model (numerical and quasi-exact analytical solution) and its comparison with those calculated from full self-consistent N-particle beam simulations.

	$r_o = 1.0$	$r_o = 1.2$	$r_o = 1.4$	$r_o = 1.6$	$r_o = 1.8$
r_c	$= 1$	$\cong 1.05$	$\cong 1.10$	$\cong 1.10$	$\cong 1.20$
r_h	$= 0$	$\cong 1.68$	$\cong 1.88$	$\cong 2.00$	$\cong 2.13$
Semicircular approximation – Numerical Solution					
f	$= 0$	$\cong 0.00566$	$\cong 0.04666$	$\cong 0.08098$	$\cong 0.13185$
r_b	$= 1$	$\cong 1.03474$	$\cong 1.11179$	$\cong 1.21944$	$\cong 1.33770$
ϵ	$= 0$	$\cong 0.27512$	$\cong 0.54021$	$\cong 0.85104$	$\cong 1.18855$
Semicircular approximation – Analytical Solution					
f	$= 0$	$\cong 0,00557$	$\cong 0,04680$	$\cong 0,08118$	$\cong 0,13212$
r_b	$= 1$	$\cong 1,03475$	$\cong 1,11194$	$\cong 1,21967$	$\cong 1,33801$
ϵ	$= 0$	$\cong 0,27515$	$\cong 0,54067$	$\cong 0,85168$	$\cong 1,18946$
Self-consistent Numerical Simulations					
f	$= 0$	$\cong 0.02080$	$\cong 0.05181$	$\cong 0.08353$	$\cong 0.13286$
r_b	$= 1$	$\cong 1.02893$	$\cong 1.08063$	$\cong 1.16717$	$\cong 1.28389$
ϵ	$= 0$	$\cong 0.23535$	$\cong 0.45312$	$\cong 0.76491$	$\cong 1.12057$

ACKNOWLEDGMENTS

This scientific research has been done with the aid of the National Centre of Supercomputation of the Brazil's South Region (CESUP), located at the Federal University of Rio Grande do Sul (UFRGS).

REFERENCES

[1] R. P. Nunes, R. Pakter, and F. B. Rizzato, Phys. Plasmas 14 (2), 023104 (2007).
[2] C. K. Allen et al., Phys. Rev. Lett. 89 (21), (2002).
[3] A. J. Lichtenberg and M. A. Lieberman, Regular and Stochastic Motion (Springer-Verlag, New York, 1992), p. 115.
[4] R. L. Gluckstern, Phys. Rev. Lett. 73, 1247 (1994).
[5] R. P. Nunes. Technical Report (2008). To be published at UFRGS.
[6] R. P. Nunes, R. Pakter, and F. B. Rizzato, J. Appl. Phys. 104 (1), (2008). To be published.
[7] R. C. Davidson and H. Qin, Physics of Intense Charged Particle Beams in High Energy Accelerators (World Scientific, Singapore, 2001), pp. 269 (Energy Conservation).
[8] M. Benammar, IEEE Transactions on Circuits and Systems, 52 (2), (2005).